Application of HPLC in Disposition Study of A14-^{125}I-Labeled Insulin in Mice

HITOSHI SATO, AKIRA TSUJI, KEN-ICHI HIRAI, AND YOUNG SOOK KANG

To describe quantitatively the in vivo distribution and elimination of insulin, high-performance liquid chromatography (HPLC) separation was applied to the pharmacokinetic study of human insulin labeled with ^{125}I at tyrosine A14 (A14-^{125}I-insulin) as a tracer. Intact A14-^{125}I-insulin levels were determined by HPLC and trichloroacetic acid (TCA) precipitation in plasma and various tissues after its intravenous bolus injection into mice. TCA precipitation consistently overestimated the intactness of A14-^{125}I-insulin compared with HPLC, possibly due to the presence of both a TCA-precipitable intermediate degradation product of labeled insulin found in HPLC elution profiles and reported high-molecular-weight forms of labeled insulin in plasma. Thus, TCA precipitation gave a considerably lower total plasma clearance (Cl_{tot}) value than HPLC. The half-life of A14-^{125}I-insulin was prolonged by a simultaneous injection of 8 U/kg unlabeled insulin, and labeled insulin behaved similarly to [^{14}C]inulin (an extracellular fluid marker). The concentration time profiles of HPLC-separated labeled insulin in plasma were analyzed by a noncompartmental moment method, and both Cl_{tot} and steady-state apparent volume distribution (VD_{ss}) of A14-^{125}I-insulin were considerably decreased by unlabeled insulin coadministration. In particular, VD_{ss} of labeled insulin decreased by 79%, similar to that of inulin (181 ml/kg), suggesting that the nonspecific binding of labeled insulin to tissues was so small that VD_{ss} of labeled insulin was reduced to the extracellular fluid volume (~20% of the body weight) when its receptor binding was blocked effectively by unlabeled insulin. This observation, together with the 63% reduction of Cl_{tot} by unlabeled insulin coadministration, demonstrated that saturable, receptor-mediated processes of distribution and elimination are essentially involved in the pharmacokinetics of HPLC-separated A14-^{125}I-insulin. *Diabetes* **39:563–69, 1990**

From the Department of Pharmaceutics, Faculty of Pharmaceutical Sciences, Kanazawa University, Kanazawa, Japan.

Address correspondence and reprint requests to Prof. Akira Tsuji, PhD, Faculty of Pharmaceutical Sciences, Kanazawa University, Takara-machi 13-1, Kanazawa 920, Japan.

Received for publication 3 April 1989 and accepted in revised form 4 January 1990.

High-performance liquid chromatography (HPLC) has been successfully employed not only to purify authentic insulin (1) and monoiodinated insulin isomers (2,3) but also to separate the degradation products of labeled insulin generated by isolated hepatocytes (4,5) or proteases (5,6). Previous in vitro studies indicated that trichloroacetic acid (TCA)-precipitable, insulin-sized intermediate products of insulin appear to be derived from cell-associated processes (4–9). After degradation by human fibroblasts, separation of insulin-sized products of insulin was readily accomplished by HPLC but not by other methods (9). In contrast, many in vivo kinetic studies of insulin have been performed almost exclusively by radioimmunoassay (RIA), gel filtration, and TCA precipitation but have not been evaluated quantitatively by HPLC analysis.

In the field of pharmacokinetics, there is a growing body of evidence demonstrating the important roles of receptor binding in distribution and elimination of peptide hormones (10–12), including insulin (13–15), due to hormone-receptor binding and subsequent cellular events (receptor-mediated internalization and degradation) that have been studied extensively with isolated cells (16,17). With regard to the receptor binding activity of radiolabeled insulin, it has been reported that HPLC-purified A14-[^{125}I]monoiodoinsulin is indistinguishable from native insulin (18) and that B-chain–labeled insulins show higher affinity than A14-[^{125}I]monoiodoinsulin in adipocytes, possibly due to the alterations in either receptor binding or cooperative interactions, because tyrosines of the B-chain are believed to be close to or within the binding site (19). However, most previous studies of the fate of labeled insulin were performed with heterogenously labeled insulins, except for Philippe et al. (14), who used tritiated insulin assayed by gel chromatography, and Cockram et al. (20), who utilized A14- and B1-labeled insulin tracers to investigate the mechanisms of

intracellular processing of insulin in vivo by TCA precipitation and immunoprecipitation, although they did not directly measure the intracellular degradation products of insulin.

In this study, we quantitatively compared the intactness of insulin labeled with ^{125}I tyrosine A14 (A14-^{125}I-insulin) between the HPLC-separation and TCA-precipitation methods and examined the concentration profiles of HPLC-separated A14-^{125}I-insulin in plasma and various tissues after its intravenous injection in mice.

RESEARCH DESIGN AND METHODS

Human A14-^{125}I-insulin with a specific activity of 2000 Ci/mmol and [^{14}C]inulin carboxylic acid with a specific activity of 2–10 mCi/mmol were purchased from the Radiochemical Center (Amersham, Arlington Heights, IL). Crystalline pork insulin and bovine serum albumin (fraction V) were obtained from Sigma (St. Louis, MO), and TCA and trifluoroacetic acid were from Wako (Osaka, Japan). All other reagents were commercially available and of analytic grade. The monoiodinated insulin was dissolved in phosphate-buffered saline (PBS) containing 0.1% bovine serum albumin (PBS solution) and stored at −20°C until study. The purity of the labeled insulin was at least 95% as assayed by HPLC.

Insulin administration and sampling. Adult male ddY mice (Sankyo, Toyama, Japan) weighing 30–38 g were used throughout the experiments without fasting. Under light anesthesia with ether, the mice were kept in the supine position on a fixed board, and body temperature was maintained at 37°C by heating lamps. The jugular vein was cannulated with polyethylene tubing (SP-10, OD 0.61 mm, ID 0.28 mm; Natsume Seisakusho, Tokyo) for administration of labeled insulin, and a loose ligature (surgical string) was placed around the carotid artery for blood sampling. After recovery from anesthesia, 6.5 μCi/kg of A14-^{125}I-insulin (with and without 8 U/kg unlabeled pork insulin) plus saline up to 50 μl was rapidly injected through the jugular vein with a microsyringe attached to the cannula. When unlabeled insulin was coadministered, glucose was constantly infused at a rate of 24 mg · min^{-1} · kg^{-1} to maintain euglycemia. At designated times after intravenous injection of labeled (and unlabeled) insulin, the carotid artery was gently pulled upward with the string and dissected for collection of blood into heparinized tubes, from which plasma was separated by centrifugation. The liver, kidney, lung, spleen, and gut (first third of the small intestine) were quickly excised, rinsed with ice-cold saline, and blotted dry. Each tissue was precisely weighed and quickly added to 1 ml ice-cold 1 M acetic acid solution containing 6 M urea (AcOH solution). After total ^{125}I radioactivity was counted in a γ-counter (ARC-605, Aloka, Tokyo), each tissue was homogenized in a motor-driven Potter homogenizer at 4°C. The tissue homogenates were then centrifuged at 12,000 rpm for 20 min in a microcentrifuge (MR-15A, Tomy Seiko, Tokyo) at 4°C, and the supernatants (designated tissue samples) were transferred to separate tubes. The radioactivity recovered in the supernatant was >80% of the total radioactivity. A14-^{125}I-insulin in plasma and tissue samples was assayed by the TCA-precipitation or HPLC method as described later. Plasma glucose concentrations were measured by a glucose peroxidase method (21) with a commercial kit (Glucose B-Test, Wako). Plasma insulin concentrations were determined by RIA with a commercial kit (Eiken, Tokyo).

To compare the pharmacokinetic behavior between insulin and inulin (an extracellular fluid marker), [^{14}C]inulin (30 μCi/kg), which has a molecular weight (5200 M_r) close to insulin, was intravenously injected through the cannulated jugular vein, and blood was sampled at designated times, as performed previously in rats (22) and rabbits (23). The obtained plasma samples were oxidized with a sample oxidizer (ASC-113, Aloka) to $^{14}CO_2$, and radioactivity was determined by a liquid-scintillation counter (LSC-700, Aloka).

Analytic procedures. Intactness of A14-^{125}I-insulin in plasma and various tissues was determined by TCA precipitation and HPLC as follows. For TCA precipitation, plasma samples (100 μl) were mixed well with 1 ml 5% (wt/vol) TCA aqueous solution. Similarly, tissue samples (1 ml) were mixed well with an equal volume of 10% (vol/vol) TCA aqueous solution. These mixtures were kept standing at 4°C for 30 min and then centrifuged at 1500 × *g* for 15 min, and the supernatant was transferred to a separate tube by aspiration. The percentage of radioactivity in precipitate was calculated as

$$\frac{\text{counts per min (cpm) in precipitate}}{(\text{cpm in precipitate} + \text{cpm in supernatant})100}$$

For HPLC, plasma samples (100 μl) were mixed vigorously with an equal volume of ethanol and centrifuged at 10,000 × *g* for 20 min in a microcentrifuge (MR-15A), and the supernatant was filtered through a filter (0.45 μm, Nihon Millipore Kogyo, Yonezawa, Japan). The percent of the radioactivity extracted from the samples by ethanol was ~90%. Fifty microliters of the resultant supernatant was loaded onto a reverse-phase HPLC column (μ-Bondapak C-18, 30 cm × 3.9 mm ID; Waters, Milford, MA). The constant-flow solvent-delivery system (LC-6A, Shimadzu, Kyoto, Japan) was equipped with an ultraviolet detector (SPO-6A, Shimadzu) and a gradient programmer (SCL-6A, Shimadzu). A guard column (Corasil C-18, Waters) was placed between the injector and the analytic column. The mobile phase consisted of two solvents. Solvent A was a mixture of water and trifluoroacetic acid 0.1% (vol/vol), and solvent B was a mixture of acetonitrile and trifluoracetic acid 0.1% (vol/vol). After an isocratic run at 25% solvent B for 5 min, a linear gradient was run from 25 to 40% solvent B for 10 min, and 40% solvent B was held for 15 min. The solvent flow rate was 1 ml/min. The column and solvents were kept at room temperature. The radioactivity in each sample (1 ml) was counted in a γ-counter.

Tissue samples (homogenate supernatants) were lyophilized and reconstituted in ~200 μl of a mixture of acetonitrile and water (25:75 vol/vol). Subsequent procedures were as described above for plasma samples.

The percentage of the radioactivity associated with intact A14-^{125}I-insulin in plasma and tissue samples was calculated by measuring the peak areas eluted from the column. The total radioactivity eluted from the column was >90% of the radioactivity loaded onto the column.

Data analysis. The percentage of intact A14-^{125}I-insulin in plasma and tissue samples was expressed in terms of HPLC

by the relationship between the TCA-precipitation and HPLC methods. Plasma concentrations of A14-^{125}I-insulin and [^{14}C]inulin were expressed as percentage of dose per milliliter of plasma. Plasma concentrations of labeled insulin were calculated by

$$\frac{(\text{total cpm/ml plasma}) \times \%\ \text{intact insulin in plasma}}{\text{dose}} \Big/ 100$$

where dose is intact cpm administered divided by body weight in kilograms.

Plasma concentration versus time curves of A14-^{125}I-insulin and [^{14}C]inulin were analyzed by a noncompartmental moment method (24). Total plasma clearance (Cl_{tot}) and the steady-state apparent volume distribution (VD_{ss}) were calculated by

$$Cl_{tot} = \frac{\text{dose}}{AUC}$$

$$VD_{ss} = \frac{\text{dose AUMC}}{AUC^2}$$

where AUC and AUMC are the area under the plasma concentration curve versus time curve and the area under the product of time curve and the plasma concentration versus time curve, respectively. AUC and AUMC were calculated by the trapezoidal rule with extrapolation to infinite time (24). Cl_{tot} and VD_{ss} of A14-^{125}I-insulin and [^{14}C]inulin were compared by one-way analysis of variance followed by Student's *t* test among three groups of mice injected with a tracer dose of A14-^{125}I-insulin, a tracer dose of A14-^{125}I-insulin with 8 U/kg unlabeled insulin, or a tracer dose of [^{14}C]inulin.

RESULTS

Figure 1*A* shows a representative HPLC elution profile of standard A14-^{125}I-insulin and indicates that the monoiodinated insulin used was a highly purified preparation. Figure 1, *B–D*, shows representative HPLC elution profiles of A14-^{125}I-insulin and its degradation products from plasma, kidney, and liver 15 min after intravenous bolus injection into mice. Among the major three peaks of radioactivity observed, the first peak probably corresponds for the most part to ^{125}I$^-$ and in part to ^{125}I-labeled tyrosine in view of the findings of Sodoyez et al. (25), whose studies demonstrated a very rapid dehalogenation of ^{125}I-labeled tyrosine in vivo. The second

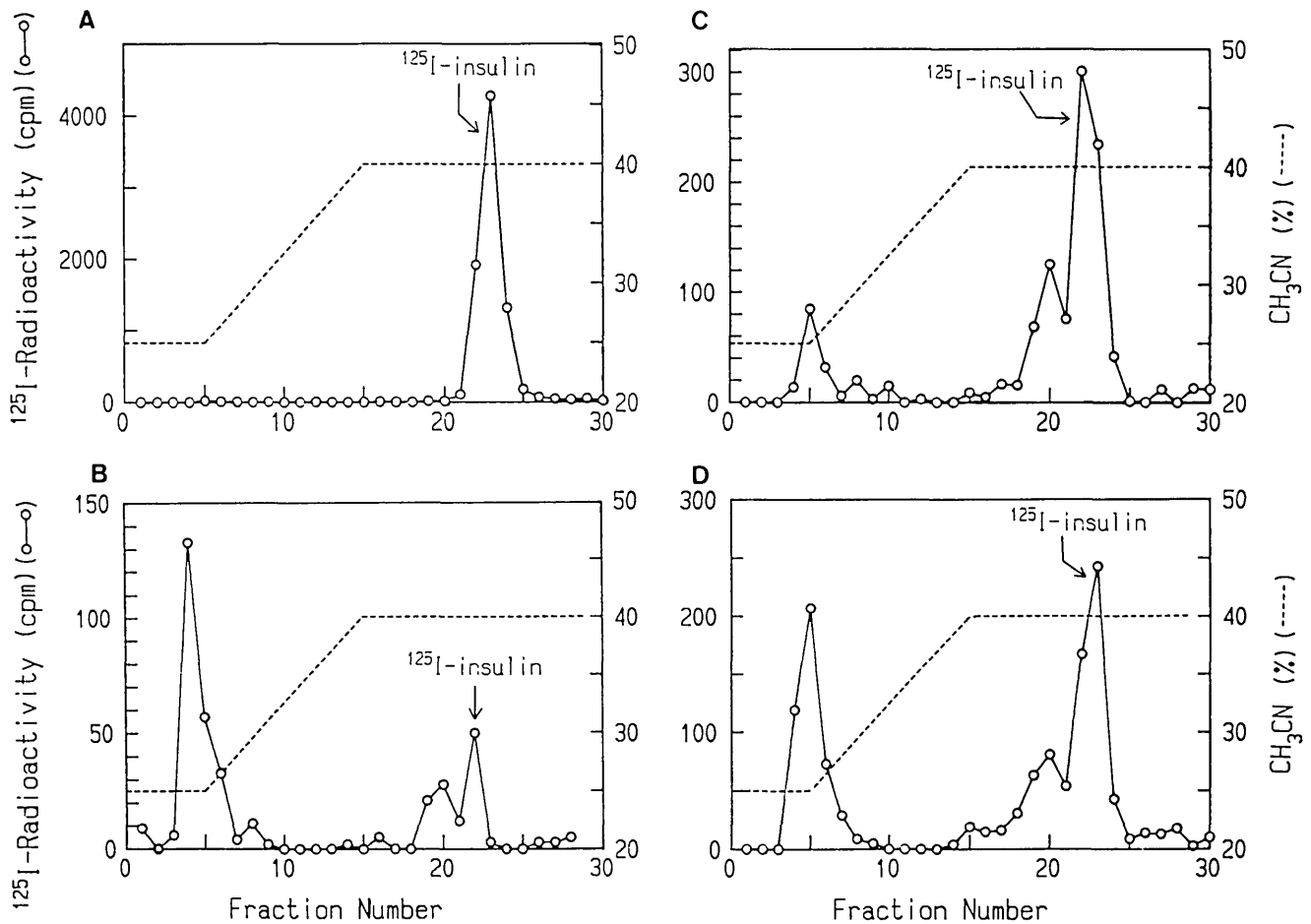

FIG. 1. Representative high-performance liquid chromatography elution profiles of A14-^{125}I-labeled insulin in standard A14-^{125}I-insulin (*A*), plasma (*B*), and tissue samples from kidney (*C*) and liver (*D*). Plasma and tissues were taken from mice 15 min after intravenous injection of A14-^{125}I-insulin (6.5 μCi/kg). For details of sample pretreatment, see text. ○, ^{125}I radioactivity (counts/min [cpm]) in 1-ml fractions eluting from μ-Bondapak C-18 column with acetonitrile gradient shown by *dashed lines*. Flow rate was set at 1 ml/min. For other chromatography conditions, see text.

peak corresponds to an intermediate degradation product of labeled insulin and the third to intact A14-^{125}I-insulin.

Figure 2 illustrates a curvilinear relationship of the percentage of intact labeled insulin between the TCA-precipitation and HPLC-separation methods. It indicates that TCA precipitation consistently overestimates the intactness of A14-^{125}I-insulin in plasma and tissues, possibly due to the nonspecific adsorption of TCA-soluble fragments including ^{125}I-labeled iodide to the pellet or due to the presence of an intermediate degradation product (Fig. 1, *B–D*), which was ~80% precipitable by 5% TCA. There was a decrease with time in the peak area associated with A14-^{125}I-insulin and a corresponding increase in the area of the first peak, and therefore, the intactness of A14-^{125}I-insulin decreased with time in plasma and tissues after its intravenous injection (Fig. 2). By utilizing this correlation between the two methods, it was clearly shown that the AUCs of HPLC-separated A14-^{125}I-insulin after its intravenous injection (Fig. 3*B*) distinctly differed from the AUCs of TCA-precipitable A14-^{125}I-insulin (Fig. 3*A*). With a noncompartmental moment analysis (24), Cl_{tot} and VD_{ss} of TCA-precipitable A14-^{125}I-insulin were determined to be 3.06 ml · min^{-1} · kg^{-1} and 1332 ml/kg, respectively. On the other hand, Cl_{tot} and VD_{ss} of HPLC-separated A14-^{125}I-insulin were determined to be 45.1 ml · min^{-1} · kg^{-1} and 1204 ml/kg, respectively (Table 1). Thus, the TCA-precipitation method gave a considerably lower Cl_{tot} and a slightly higher VD_{ss} than the HPLC method.

Mean ± SE basal glucose and insulin concentrations in plasma were 14.4 ± 0.78 mM (n = 11) and 281.4 ± 35.9 pM (n = 11), respectively. With glucose infusion, plasma glucose levels after 30 min in mice injected with 8 U/kg unlabeled insulin were not significantly different from those in mice injected with tracer insulin injection, although it was not confirmed whether this euglycemic condition was continuously maintained throughout the experiment. However, from the observation that high doses of insulin behaved similarly to inulin (Fig. 3, *B* and *C*), which is an extracellular marker as verified previously in rats (22) and rabbits (23), it is likely that the in vivo receptor binding of A14-^{125}I-insulin was almost completely displaced by a high dose of unlabeled insulin. Therefore, possible alterations in endogenous insulin secretion, caused by either hyperglycemia or hypoglycemia during intravenous glucose infusion after unlabeled insulin injection will not affect the pharmacokinetics of A14-^{125}I-insulin in this condition.

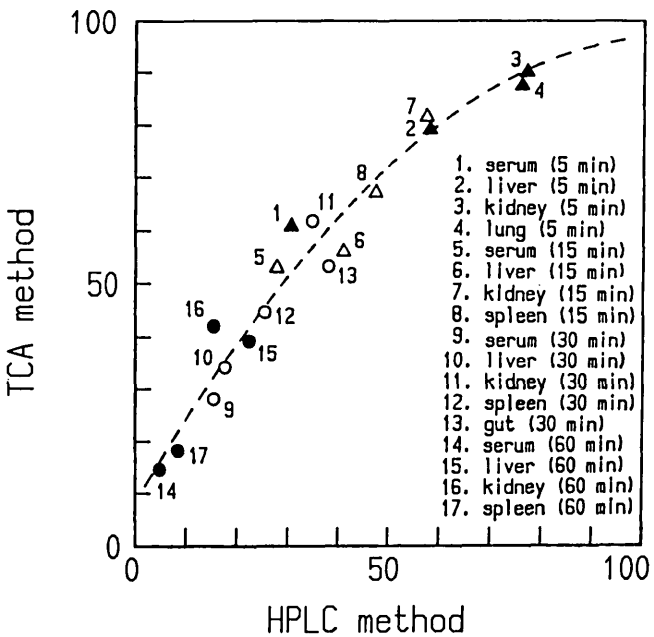

FIG. 2. Relationship of percentage of intact A14-^{125}I-labeled insulin in trichloroacetic acid (TCA) precipitation and high-performance liquid chromatography (HPLC) methods in plasma and tissue samples obtained 5 (▲), 15 (△), 30 (○), and 60 (●) min after intravenous injection in mice. After pretreatment procedure, percentage of intact insulin in each plasma or tissue sample (numbered 1–17) was determined by both TCA precipitation and HPLC. Note that TCA precipitation consistently overestimates percentage of intact labeled insulin in biological samples compared with HPLC.

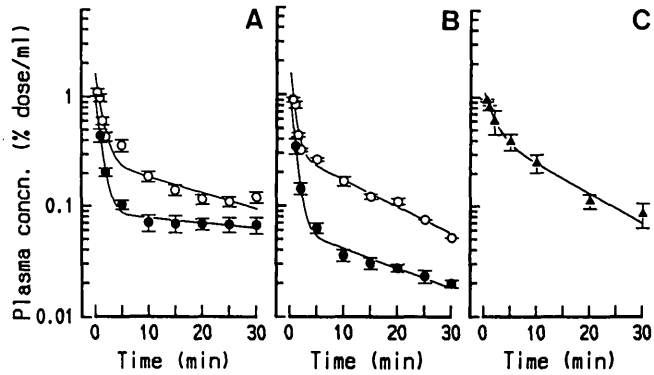

FIG. 3. Plasma disappearance curves of trichloroacetic acid–precipitable A14-^{125}I-labeled insulin (*A*) and high-performance liquid chromatography–separated A14-^{125}I-insulin (*B*) after intravenous bolus injection (6.5 μCi/kg) with (○) and without (●) simultaneous injection of 8 U/kg unlabeled insulin in mice. Disappearance of [^{14}C]inulin (30 μCi/kg) from plasma (▲) is also presented (*C*). Each *point* with *vertical bar* is mean ± SE (n = 3–5).

The plasma concentrations of HPLC-separated A14-^{125}I-insulin and [^{14}C]inulin were analyzed by a noncompartmental moment method (24), and the obtained pharmacokinetic parameters (Cl_{tot} and VD_{ss}) are listed in Table 1. Here, the extrapolation of observed data to infinite time was performed to evaluate the terminal slope by a least-squares regression line generated from the data points over 10–30 min. Analysis of variance indicated that the differences in Cl_{tot} and VD_{ss} among the three AUCs in mice were significant at the 1% level. Cl_{tot} (16.5 ml · min^{-1} · kg^{-1}) and VD_{ss} (251 ml/kg) of labeled insulin at the high dose were considerably lower than

TABLE 1
Total body clearance (Cl_{tot}) and steady-state apparent volume distribution (VD_{ss}) of A14-^{125}I-labeled insulin and [^{14}C]inulin in mice

Tracer	Cl_{tot} (ml · min^{-1} · kg^{-1})	VD_{ss} (ml/kg)
A14-^{125}I-insulin		
Tracer dose (6.5 μCi/kg)	45.1 ± 3.1	1204 ± 195
Plus 8 U/kg unlabeled insulin	16.5 ± 0.4*	251 ± 13*
[^{14}C]inulin (30 μCi/kg)	11.3 ± 1.5	181 ± 62

Values are means ± SD. Cl_{tot} and VD_{ss} were determined by a noncompartmental analysis with plasma concentrations (n = 3–5 for each data point) of A14-^{125}I-insulin and [^{14}C]inulin after intravenous injection as described in RESEARCH DESIGN AND METHODS.
*P < 0.01 vs. tracer dose of insulin.

those of tracer insulin but similar to those of [^{14}C]inulin (11.3 ml · min^{-1} · kg^{-1} and 181 ml/kg, respectively; Table 1). Student's *t* test at the 1% significance level revealed that Cl_{tot} and VD_{ss} values were significantly different between any combinations of the three groups, except that VD_{ss} values were not significantly different between the mice injected with A14-^{125}I-insulin at a high dose of unlabeled insulin and those injected with [^{14}C]inulin.

DISCUSSION

The close correlation between receptor binding activity and the extent of elimination and tissue distribution after intravenous administration has been demonstrated for some peptide hormones, including insulin (10–15). This correlation should be considered in pharmacokinetic studies of endogenous peptides and proteins because of two possible consequences: *1*) a tracer with decreased affinity shows decreased distribution volumes and plasma clearances, and *2*) a tracer with high affinity shows dose-dependent nonlinear pharmacokinetics at doses that saturate its receptors, whereas a tracer with low affinity shows dose-independent linear pharmacokinetics. Unfortunately, differences in the affinity of tracers and the doses of insulin (or plasma insulin levels) together with differences in assay methods have made it difficult to comprehensively integrate much pharmacokinetic information on the distribution volume and clearance values of insulin reported previously from different laboratories.

In this study, a rapid-HPLC method was applied to the study of in vivo distribution and elimination of A14-^{125}I-insulin in mice. The use of tracer with a high specific activity enabled us to examine the disposition of exogenously administered insulin with no interference from endogenous insulin in plasma and tissues. Moreover, the A14-[^{125}I]monoiodoinsulin used was reported to show equipotency with native insulin in isolated adipocytes (18). Thus, the distribution and elimination of A14-^{125}I-insulin (without unlabeled insulin injection) could be the consequence of physiological interactions of labeled insulin with its receptors and degradation enzymes in target tissues such as liver, muscle, and adipose tissue.

Previous in vitro studies found that TCA-precipitable insulin-sized intermediate products of insulin were generated by the interaction of insulin with degrading proteases in cytosol (4–6) and on the external surface of the cell membrane (7–9). Among the assay methods of endogenous and exogenous insulins, RIA recognizes a certain immunoreactive portion of the insulin molecule, so that it cannot distinguish between intact insulin and intermediate products of insulin. Similarly, the TCA-precipitation method, although very rapid and easy to carry out, recognizes various-sized fragments of peptides that can be precipitable in TCA solution, so that it cannot separate high-molecular-weight forms and intermediate products of insulin from intact insulin. Because high-molecular-weight radioactive insulin exhibited a prolonged half-life compared with monocomponent insulin (26), it follows that TCA precipitation inevitably gives small values of Cl_{tot} and VD_{ss} of A14-^{125}I-insulin compared with [^{14}C]inulin (Fig. 3) despite the fact that insulin is eliminated from plasma not only by renal glomerular filtration but also by metabolism by liver and muscle under physiological conditions (27). Moreover, TCA precipitation gave Cl_{tot} values of A14- and B1-labeled insulin tracers approximately half of those obtained by immunoprecipitation in dogs (20), suggesting the presence of insulin molecular fragments that retain little immunoreactivity but high TCA precipitability because of sufficient molecular size. These lines of evidence lend proof to the lack of reliability to estimate the Cl_{tot} and VD_{ss} values of labeled insulin by the use of TCA-precipitation method.

In in vitro experiments, separation of the various fragments of insulin, particularly insulin-sized products, can be readily accomplished by reverse-phase HPLC (6,9). In this in vivo study, the HPLC elution profiles indicate that there are at least two products of A14-labeled insulin less hydrophobic than intact insulin in plasma and tissues after intravenous injection in mice (Fig. 1, *B–D*). The peak eluting near intact insulin presumably represents insulin-sized intermediate products because it was TCA precipitable by ~80%. From this point of view, HPLC analysis appears to be more reliable than other methods for the measurement of intact A14-^{125}I-insulin in biological samples of in vivo and in vitro studies. However, because it is too laborious to analyze many biological samples by HPLC, we routinely employed the TCA-precipitation method, and then the obtained TCA precipitability was converted into the percentage of intact insulin by the HPLC method using the correlation between these two methods (Fig. 2). With this approach, a high TCA precipitability (e.g., >90%) may not cause a significant change in insulin concentrations, whereas a low TCA precipitability (e.g., <15%) may cause a wide variation in estimating the HPLC intactness from the calibration curve presented in Fig. 2. This is why we did not analyze the plasma concentrations of A14-^{125}I-insulin at >30 min after intravenous injection, when TCA precipitability of A14-^{125}I-insulin in plasma samples fell close to the unreliable lower extreme of the curve.

Because liver is the major eliminating organ of insulin in vivo, the result of HPLC separation of biological samples could be compared with that of Hamel et al. (4), who have shown by HPLC that two insulin-sized intermediate products were generated in hepatocytes incubated with A14-^{125}I-insulin at 37°C, whereas a single intermediate product was found in the incubation medium. In contrast, in this study, only one intermediate product of A14-^{125}I-insulin was separated by HPLC from the liver and plasma samples (Fig. 1). This may be because the retention time of labeled insulin in this study (23 min) was so short compared with that in the study of Hamel et al. (55 min) that our HPLC analysis could not detect "doublets," pairs of insulin-sized material that eluted from their HPLC system in close positions (at 19 and 23 min). However, considering that some degradation occurs on the membrane (28), we cannot exclude the possibility that one of the above-mentioned doublets is ascribed to extracellular degradation, and the generated intermediate product was washed out from the extracellular space by the rapid blood flow before partitioning into hepatocytes, whereas even a slow uptake of the product by hepatocytes may proceed in in vitro conditions where cells are surrounded by the same incubation medium.

The good recovery (>80%) of A14-^{125}I-insulin from tissues (in 1 M AcOH solution and 6 M urea) may be explained not only by the effects of low pH and urea in homogenates, which effectively dissociate insulin from its receptors (29), but also by the effect of urea to dissociate degraded insulin fragments

noncovalently bound to certain tissue components, as previously demonstrated for ^{125}I-labeled nerve growth factor (30). TCA precipitabilities of labeled insulin in the pellets were almost equal to those in the supernatants after centrifugation of tissue homogenates in AcOH solution, suggesting that, at most, 20% loss of radioactivity during the extraction from tissue samples was not due to specific binding of labeled insulin to certain cellular components but to nonspecific adsorption to the pellets. In this study of rapid HPLC analysis, we preferred a simple method of extraction of radioactive materials to other procedures that may give consistently higher yields. Moreover, because ethanol does not precipitate free insulin but insulin-receptor complexes (31), it is reasonable that A14-^{125}I-insulin was recovered well after tissue homogenates were deproteinized with ethanol in the presence of urea at a low pH (in acetic acid). Taken altogether, the good recovery of labeled insulin in the above pretreatment procedures made it possible to quantitatively evaluate the in vivo disposition of insulin by HPLC.

The large VD_{ss} value (~120% of body wt) of A14-^{125}I-insulin at a tracer dose suggests that insulin is not only distributed to the extracellular fluid but also reversibly bound to its binding sites (receptors) in target tissues at the physiological concentrations of plasma insulin. In contrast, when a high dose of unlabeled insulin was simultaneously injected, A14-^{125}I-insulin behaved similarly to [^{14}C]inulin (Fig. 3). Pharmacokinetic analysis revealed that VD_{ss} of labeled insulin decreased significantly by 79% with a simultaneous injection of 8 U/kg unlabeled insulin to be close to that of inulin (181 ml · min^{-1} · kg^{-1}), suggesting that the nonspecific binding of labeled insulin to tissues was so small that VD_{ss} of labeled insulin was reduced to the extracellular fluid volume (~20% of body wt) when its receptor binding was blocked effectively by unlabeled insulin. Moreover, Cl_{tot} of insulin was reduced significantly by 63% with a simultaneous injection of unlabeled insulin but was somewhat higher (11.3 ml · min^{-1} · kg^{-1}) than that of [^{14}C]inulin because of the presence of certain nonspecific clearance mechanisms other than renal glomerular filtration, which coincides with the presence of non–receptor-mediated clearance found in isolated rat hepatocytes (17). A very similar result was reported in rats for the initial volume distribution and metabolic clearance of [^{3}H]insulin assayed by gel chromatography (14). From the above findings, it was demonstrated that saturable and receptor-mediated processes at tissue distribution and elimination are involved in the pharmacokinetics of HPLC-separated A14-^{125}I-insulin. The results obtained by HPLC will be important in relating these in vivo pharmacokinetic processes to the physiological and biochemical consequences in a quantitative manner, e.g., transcapillary diffusion, receptor binding, internalization with receptors, and intracellular degradation.

In conclusion, HPLC was applied to the pharmacokinetic study of insulin in mice with A14-^{125}I-insulin as a tracer, which retains the same receptor binding activity and biological potency as native insulin. HPLC elution profiles from plasma and tissues indicated the presence of at least two products of insulin in plasma and tissues more hydrophilic than intact insulin, and TCA-precipitable material, which eluted close to intact insulin, might be one of the insulin-sized intermediate products reported in previous in vitro studies with isolated hepatocytes and adipocytes. Further characterization of the radioactivity associated with each peak would give more information on the mechanisms of intracellular processing of insulin in vivo, but this is beyond the scope of this study. Accordingly, this must be viewed as a first step of HPLC application to the study of in vivo disposition of insulin.

ACKNOWLEDGMENTS

This study was supported by a grant-in-aid for scientific research from the Ministry of Education, Science, and Culture of Japan; the Project Research Fund from the Graduate School of Natural Science and Technology, Kanazawa University; and grants from Takeda Science Foundation and Nakatomi Health Science Foundation.

REFERENCES

1. Johnson IS: Authenticity and purity of human insulin (recombinant DNA). *Diabetes Care* 5 (Suppl. 2):4–12, 1982
2. Stenz FB, Wright RK, Kitabchi AE: A rapid means of separating A14-^{125}I-insulin from heterogeneously labeled insulin molecules for biologic studies. *Diabetes* 31:1128–31, 1982
3. Frank BH, Peavy DE, Hooker CS, Duckworth WC: Receptor binding properties of monoiodotyrosyl insulin isomers purified by high performance liquid chromatography. *Diabetes* 32:705–11, 1983
4. Hamel FG, Peavy DE, Ryan MP, Duckworth WC: HPLC analysis of insulin degradation products from isolated hepatocytes. *Diabetes* 36:702–708, 1987
5. Duckworth WC, Hamel FG, Peavy DE, Liepnieks JJ, Ryan MP, Hermodson MA, Frank BH: Degradation products of insulin generated by hepatocytes and by insulin protease. *J Biol Chem* 263:1826–33, 1988
6. Hamel FG, Peavy DE, Ryan MP, Duckworth WC: High performance liquid chromatographic analysis of insulin degradation by rat skeletal muscle insulin protease. *Endocrinology* 118:328–33, 1986
7. Blackard WG, Ludeman C, Stillman J: Role of hepatocytes plasma membrane in insulin degradation. *Am J Physiol* 248:E194–202, 1985
8. Sonne O: Receptor-mediated degradation of insulin in isolated rat adipocytes: formation of a degradation product slightly smaller than insulin. *Biochim Biophys Acta* 927:106–11, 1987
9. Stenz FB, Harris HL, Kitabchi AE: Early detection of degraded A14-^{125}I-insulin in human fibroblasts by the use of high performance chromatography. *Diabetes* 32:474–77, 1983
10. Weitzman RE, Fisher DA: Arginine vasopressin metabolism in dogs. I. Evidence for a receptor-mediated mechanism. *Am J Physiol* 235:E591–97, 1978
11. Sato H, Sugiyama Y, Sawada Y, Iga T, Hanano M: In vivo evidence for the specific binding of human β-endorphin to the lung and liver of the rat. *Biochem Pharmacol* 37:2273–78, 1988
12. Kim DC, Sugiyama Y, Satoh H, Fuwa T, Iga T, Hanano M: Kinetic analysis of in vivo receptor-dependent binding of human epidermal growth factor by rat tissues. *J Pharm Sci* 77:200–207, 1988
13. Berman M, McGuire EA, Roth J, Zeleznik AJ: Kinetic modeling of insulin binding to receptors and degradation in vivo in the rabbit. *Diabetes* 29:50–59, 1980
14. Philippe J, Halban PA, Gjinovci A, Duckworth WC, Estreicher J, Renold AE: Increased clearance and degradation of [^{3}H]insulin in streptozotocin diabetic rats: role of the insulin-receptor compartment. *J Clin Invest* 67:673–80, 1981
15. Eaton RP, Friedman N, Allen RC, Schade DS: Insulin removal in man: in vivo evidence for a receptor-mediated process. *J Clin Endocrinol Metab* 58:555–59, 1984
16. Hammonds GT, Jarett L: Lysosomal degradation of receptor-bound ^{125}I-labeled insulin by rat adipocytes: its characterization and dissociation from the short-term biologic effects of insulin. *Diabetes* 29:475–86, 1980
17. Donner DB: Receptor- and non-receptor-mediated uptake and degradation of insulin by hepatocytes. *Biochem J* 208:211–19, 1982
18. Gliemann J, Sonne O, Linde S, Hansen B: Biological potency and binding affinity of monoiodoinsulin with iodine in tyrosine A14 and A19. *Biochem Biophys Res Commun* 87:1183–90, 1979
19. Pullen RA, Lindsay DG, Wood SP, Tickle IJ, Blundell TL, Wollmer A, Krail G, Brandenburg D, Zahn H, Gilimann J, Gammeltoft S: Receptor-binding region of insulin. *Nature* (Lond) 259:369–73, 1976
20. Cockram CS, Jones RH, Boroujerdi MA, Sönksen PH: Evidence for separate handling in vivo of different regions of the insulin molecule using A14- and B1-labeled insulin tracers. *Diabetes* 33:721–27, 1984
21. Kingsley GR, Getchell G: Direct ultramicro glucose oxidase method for determination of glucose in biologic fluids. *Clin Chem* 6:465–75, 1960
22. Tsuji A, Yoshikawa T, Nishide K, Minami H, Kimura M, Nakashima E, Terasaki T, Miyamoto E, Nightingale CH, Yamana T: Physiologically based

pharmacokinetic model for β-lactam antibiotics. I. Tissue distribution and elimination in rats. *J Pharm Sci* 72:1239–51, 1983
23. Tsuji A, Nishide K, Minami H, Nakashima E, Terasaki T, Yamana T: Physiologically based pharmacokinetic model for cefazolin in rabbits and its preliminary extrapolation to man. *Drug Metab Dispos* 13:729–39, 1985
24. Yamaoka K, Nakagawa T, Uno T: Statistical moments in pharmacokinetics. *J Pharmacokinet Biopharm* 6:547–58, 1978
25. Sodoyez JC, Sodoyez-Goffaux FR, Moris YM: ^{125}I-insulin: kinetics of interaction with its receptors and rate of degradation in vivo. *Am J Physiol* 239:E3–11, 1980
26. Antoniades H: Metabolism of single-component and high-molecular-weight radioactive insulin in rats. *Endocrinology* 99:481–89, 1976
27. Bennett HPJ, McMartin C: Peptide hormones and their analogues: distribution, clearance from the circulation, and inactivation in vivo. *Pharmacol Rev* 30:247–92, 1979
28. Yokono K, Roth RA, Baba S: Identification of insulin-degrading enzyme on the surface of cultured human lymphocytes, rat hepatoma cells, and primary cultures of rat hepatocytes. *Endocrinology* 111:1102–108, 1982
29. De Meytes P, Bianco AR, Roth J: Site-site interactions among insulin receptors. *J Biol Chem* 251:1877–88, 1976
30. Siminoski K, Gonnella P, Bernanke J, Owen L, Neutra M, Murphy RA: Uptake and transepithelial transport of nerve growth factor in suckling rat ileum. *J Cell Biol* 103:1979–90, 1986
31. Frandsen EK, Bacchus RA: New, simple insulin-receptor assay with universal application to solubilized insulin receptors and receptors in broken and intact cells. *Diabetes* 36:335–40, 1987